

Evolution of an adaptive behavior and its sensory receptors promotes eye regression in blind cavefish

Yoshizawa *et al.*

RESEARCH ARTICLE

Open Access

Evolution of an adaptive behavior and its sensory receptors promotes eye regression in blind cavefish

Masato Yoshizawa^{1*}, Yoshiyuki Yamamoto², Kelly E O'Quin¹ and William R Jeffery¹

Abstract

Background: How and why animals lose eyesight during adaptation to the dark and food-limited cave environment has puzzled biologists since the time of Darwin. More recently, several different adaptive hypotheses have been proposed to explain eye degeneration based on studies in the teleost *Astyanax mexicanus*, which consists of blind cave-dwelling (cavefish) and sighted surface-dwelling (surface fish) forms. One of these hypotheses is that eye regression is the result of indirect selection for constructive characters that are negatively linked to eye development through the pleiotropic effects of Sonic Hedgehog (SHH) signaling. However, subsequent genetic analyses suggested that other mechanisms also contribute to eye regression in *Astyanax* cavefish. Here, we introduce a new approach to this problem by investigating the phenotypic and genetic relationships between a suite of non-visual constructive traits and eye regression.

Results: Using quantitative genetic analysis of crosses between surface fish, the Pachón cavefish population and their hybrid progeny, we show that the adaptive vibration attraction behavior (VAB) and its sensory receptors, superficial neuromasts (SN) specifically found within the cavefish eye orbit (EO), are genetically correlated with reduced eye size. The quantitative trait loci (QTL) for these three traits form two clusters of congruent or overlapping QTL on *Astyanax* linkage groups (LG) 2 and 17, but not at the *shh* locus on LG 13. Ablation of EO SN in cavefish demonstrated a major role for these sensory receptors in VAB expression. Furthermore, experimental induction of eye regression in surface fish via *shh* overexpression showed that the absence of eyes was insufficient to promote the appearance of VAB or EO SN.

Conclusions: We conclude that natural selection for the enhancement of VAB and EO SN indirectly promotes eye regression in the Pachón cavefish population through an antagonistic relationship involving genetic linkage or pleiotropy among the genetic factors underlying these traits. This study demonstrates a trade-off between the evolution of a non-visual sensory system and eye regression during the adaptive evolution of *Astyanax* to the cave environment.

Keywords: animal behavior, regressive evolution, constructive evolution, neuromast, hedgehog, tradeoff, quantitative trait locus, eye, QTL cluster, adaptation

Background

The dark and nutrient poor cave environment exerts substantial pressure upon cave-dwelling animals. Perhaps as a consequence of these limited resources, cave-adapted animals from most major phyla exhibit a remarkable

convergence in morphological and physiological changes related to cave life, including features that are both constructive (the lengthening of legs, fins and antennae, the appearance of novel behaviors, and elaboration of non-visual sensory systems) and regressive (the reduction or loss of vision and pigmentation) [1,2]. Although these changes have been studied in a diverse set of cave animals, the genetic and evolutionary mechanisms responsible for them remain poorly understood.

* Correspondence: yossy@umd.edu

¹Department of Biology, University of Maryland, College Park, MD 20742, USA

Full list of author information is available at the end of the article

Although natural selection is probably involved in the evolution of constructive cave adapted phenotypes [3], the evolutionary forces driving regressive changes are less certain. Darwin suggested that eye degeneration - one of the most conspicuous traits found in cave animals - evolved due to disuse [4]. This idea was refined by others to implicate neutral mutation and genetic drift as a consequence of relaxed selection for vision in the cave environment [5,6]. The neutral hypothesis was favored until recently when the results of new genetic and developmental studies supported the adaptive evolution of eye regression in cave animals. Three competing hypotheses have been proposed for the adaptive evolution of eye regression: (1) direct natural selection against eyes to conserve energy in the resource poor cave environment [7]; (2) indirect selection against eyes to open sufficient space for the elaboration of constructive characters [2,8-10]; and (3) indirect selection against eyes due to the enhancement of traits that are negatively linked to optic development by antagonistic pleiotropy [11,12]. Distinguishing among these hypotheses has been difficult since the genetic basis of eye reduction is unknown in cave-dwelling animals.

The teleost *Astyanax mexicanus* is an excellent model organism for studying the evolution of traits associated with cave life, including eye regression [5,13-16]. Within the past few million years, at least five independent colonizations by two different migrational waves of eyed surface fish have established 29 geographically isolated *Astyanax* cavefish populations in northeastern Mexico [17-20]. After subsequent radiation underground, the founder cavefish populations became isolated in separate caves and evolved eye regression, reduced pigmentation or albinism, enhanced sensory systems and behavioral changes associated with cave life [5,11,12,21-32]. Despite this isolation, *Astyanax* surface fish and cavefish are interfertile in the laboratory, allowing the evolution of constructive and regressive traits to be studied by genetic analysis.

Previous studies reported that eye degeneration in *Astyanax* is triggered by lens apoptosis and dysfunction due to expanded *sonic hedgehog* (*shh*) gene expression along the embryonic midline [25,26]. Additionally, *shh* hyper expression was shown to increase jaw width and taste bud number, and to mediate the expansion of the forebrain and hypothalamus [11,22]. In a recent study, Elipot et al. found that *shh* modifies the hypothalamic serotonergic network and increases foraging efficiency in cavefish by shifting behavior from fighting to foraging [32]. These experiments support the hypothesis that eye regression in *Astyanax* has evolved at least in part as a result of indirect selection against eyes in favor of increased feeding efficiency through pleiotropy of the *shh* genes. However, recent genetic studies have discovered 8

to 12 quantitative trait loci (QTL) involved in eye reduction in *Astyanax* cavefish [5,7,33], but none that are linked to either the *shhA* or *shhB* genes, suggesting that upstream modulators of the SHH signaling system and/or other genetic factor(s) may be important in eye regression (for review, see ref. [3]).

In the present study, we launch an alternative approach to address the evolutionary mechanisms involved in eye degeneration. Assuming a positive relationship between visual decay and the evolution of constructive changes in other sensory systems - as has been proposed by many previous investigators [2,8,10,34,35] - we investigated the genetic basis of a constructive trait, the vibration attraction behavior (VAB), to evaluate its possible relationship to eye degeneration. VAB is the swimming of cavefish toward an oscillating object, a behavior that has evolved repeatedly in different *Astyanax* cavefish populations [27,36,37] and which may be present in Amblyopsid cavefish as well [38,39]. VAB is mediated by an increase in the number and size of cranial superficial neuromasts (SN) in cavefish [27]. Although VAB is usually absent in surface fish, a small proportion of those raised in the laboratory can show a weak form of VAB. In wild populations of surface fish, VAB is presumably deleterious since it may be easily detectable by predators [40]. In contrast, VAB is adaptive in cavefish since it increases foraging in an environment devoid of light with sparse food and no macroscopic predators [27,40].

Here we report the results of genetic analyses of VAB, SN enhancement and eye size. Using this approach, we discovered that the QTL underlying VAB, a specific class of SN located within the cavefish eye orbit (EO), and reduced eyes form two distinct clusters of overlapping QTL that together explain a significant portion of the genetic variation underlying these traits. By ablation of EO SN, we discovered that these sensory receptors contribute to VAB. Moreover, by *shh* overexpression, we also showed that induction of eye degeneration in surface fish did not induce VAB or increase EO SN, suggesting that these traits are part of an antagonistic system impacting eye formation that is independent of SHH signaling, and that the extra space opened by eye regression is insufficient to promote the appearance of these constructive traits. Therefore, we propose that the adaptive evolution of VAB and EO SN enhancement has contributed to eye degeneration in *Astyanax* cavefish.

Results

A small number of genetic factors control VAB and SN number

To determine the phenotypic and genetic relationship among eye size, VAB and SN enhancement, we first estimated the number of genetic factors that control these traits. We crossed a female Texas surface fish with a

male Pachón cavefish and raised about 130 F_1 individuals. One pair of these F_1 progeny was crossed to generate 384 F_2 individuals for phenotypic and genetic analysis. We then measured the degree of VAB, SN number and size at suborbital bone 3 (SO-3 SN) [41], SN number within the eye orbit (EO) and overall eye size in each individual. The distribution of VAB and SN scores among the P_0 , F_1 and F_2 generations suggests that all four traits are heritable and controlled by one or more genetic factors (Figure 1A-D). Classic Castle-Wright estimates of the effective number of loci for VAB, SO-3 SN number and diameter, and EO SN number were 2.0 ± 1.0 , 3.9 ± 1.2 , 0.2 ± 0.1 and 20.9 ± 22.1 , respectively (mean \pm standard error of the mean, s.e.m.). However, because the F_2 individuals from this cross did not recapitulate the entire distribution of cavefish VAB phenotypes (Figure 1A), we crossed another pair of F_1 progeny from the same P_0 to generate an additional F_2 family. We used marker-assisted selection to choose three pairs of F_2 individuals from this family that were hetero- or homozygous for cavefish alleles at two putative VAB and three SO-3 SN QTL loci (see Methods). We then crossed these F_2 in order to generate 91 F_3 individuals that recovered the entire cavefish VAB phenotype, although the distributions for SO-3 and EO SN remain somewhat restricted (Figure 1A-D). In combination with the original 384 F_2 , these additional F_3 were included to increase our ability to detect correlations and QTL for the VAB, SN and eye size phenotypes.

VAB and eye size are strongly correlated with EO SN but not SO-3 SN

Since SN are the sensory receptors that facilitate VAB [27], we expected the number of SN to be strongly correlated with the level of VAB in our hybrid families. In a previous study using cavefish, surface fish and their F_1 progeny, we found a significant positive correlation between VAB and the number of SN at SO-3, which are located in the cranial region immediately ventral to the EO [27]. However, in the present study using both F_2 and F_3 hybrids, we found that the correlation between these two traits was not significant ($r = 0.13$, $P = 0.052$; Figure 1G), although the correlation between VAB and SN diameter at SO-3 was significant ($r = 0.14$, $P = 0.044$; Figure 1H). This new result suggests that the number of SN at SO-3 may not be the most important parameter determining VAB. After further examination of SN within the cranial regions of surface fish and cavefish, we found that SN are located in the EO in cavefish (yellow dotted line in the bottom of Figure 1N) and in F_2 and F_3 hybrids with reduced eyes, but not in surface fish (yellow arrow in the bottom of Figure 1L, M; F_3 ; Figure 1K: surface fish). In contrast to the results for SO-3 SN, we found that the number of EO SN was positively correlated with VAB ($r = 0.29$, $P < 0.001$;

Figure 1F) and negatively correlated with eye size ($r = -0.44$, $P < 0.001$; Figure 1J), and that eye size was also negatively correlated with VAB ($r = -0.26$, $P < 0.001$; Figure 1I). These results suggest that VAB may be mediated by an increase in EO SN and that both traits are negatively correlated with eye size.

Genetic linkage mapping and QTL analysis

To determine the number and position of the genetic loci controlling VAB, SN number and eye size, we first constructed a genetic linkage map of the *Astyanax* genome from 246 markers genotyped among 384 F_2 individuals. Most of the markers represent randomly-distributed microsatellite polymorphisms, but we also included 28 markers representing candidate genes for SN development, behavioral variation and other previously mapped traits (for example, *ngn1*, *eya1*, *nrg2*, the *5ht* serotonin receptors, the *mao* serotonin enzyme, the *sert* serotonin transporter, *shh*, *pax6* and *oca2*) [7,23,42]. Our linkage map recovered 27 linkage groups (LG) spanning 1,513 cM (Figure 2). Since *Astyanax* have 25 haploid chromosomes [43], this map likely covers the entire genome. Our map is comparable to a previously published *Astyanax* genetic map [23] constructed from a cross between a Mexican surface fish and Pachón cavefish. Small discrepancies in marker order and inter-marker distance between this previous map and ours are likely due to the use of different surface fish populations.

Using this linkage map, we performed three types of QTL scans: (1) classic interval mapping with a single-QTL model treating the F_2 and F_3 separately, as well as combining these F_2 and F_3 datasets; (2) a modified single-QTL analysis using both F_2 and F_3 but accounting for kinship among these generations in QTLRel [44]; and (3) multiple QTL mapping with both F_2 and F_3 as implemented by the function *stepwiseqtl* in R/qtl [45,46]. By comparing the results of the first and second analyses (Additional file 1, the left and right column), we assessed the consistency of our QTL scans as well as the potential noise caused by using multiple generations. If the results were similar and relatively unaffected by kinship (see variance components in Additional file 2), we then applied the multiple QTL scan in *stepwiseqtl* since our Castle-Wright estimates suggest that a minimum of two or more loci control most traits (see above). We analyzed six traits using the classic and modified single-QTL models (VAB, SO-3 SN number, SO-3 SN diameter, EO SN number, eye size/SL and, as a control, albinism). We found similar results for all traits except SO-3 SN number and diameter (Additional file 1D, E). These two traits exhibited large variance components due to kinship and we thus dropped them from further analysis. The variance components of the remaining traits were small (Additional file 2). Using *stepwiseqtl* with both F_2 and F_3 to analyze albinism and eye size, we were able to detect two previously-reported

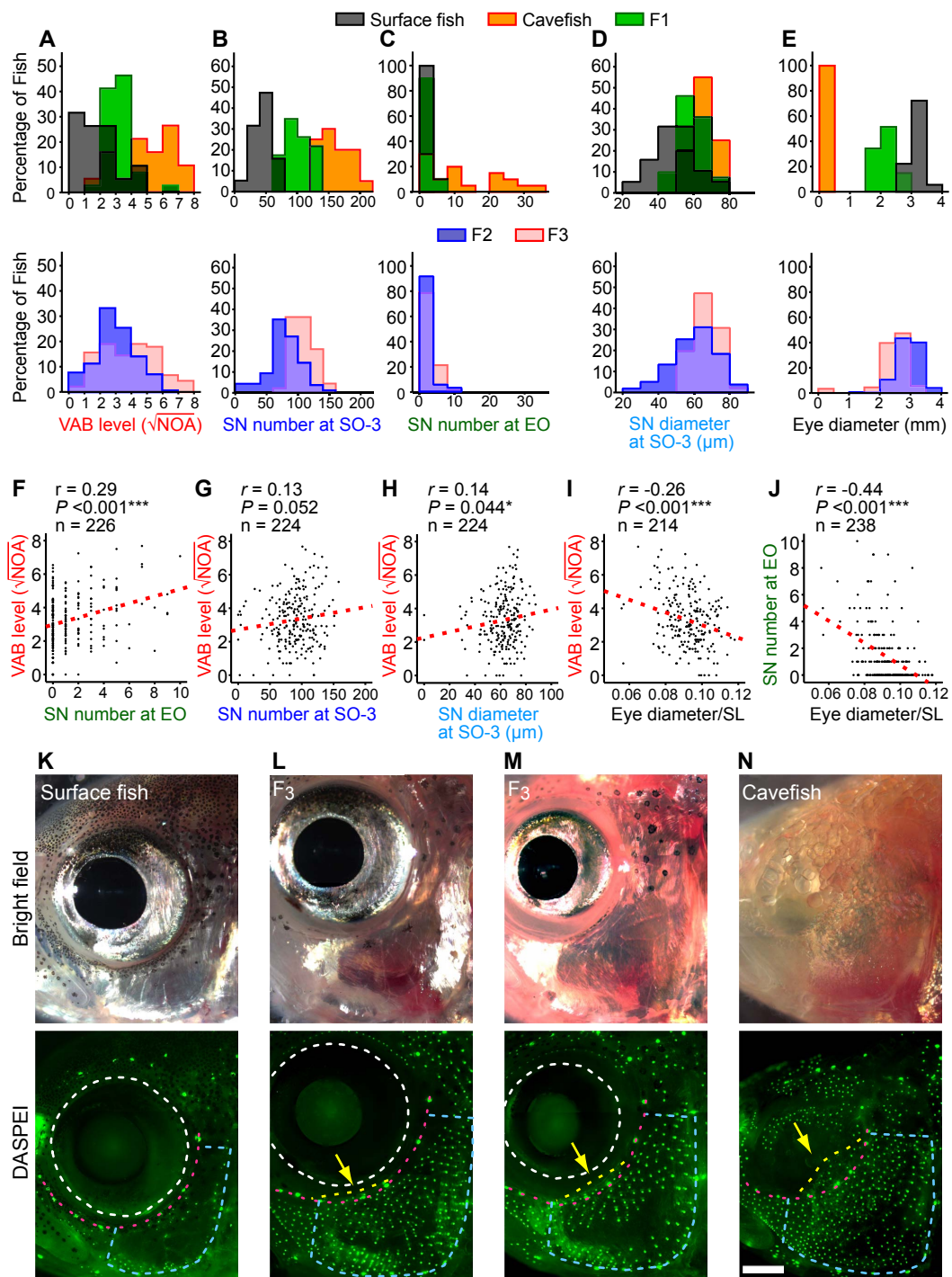
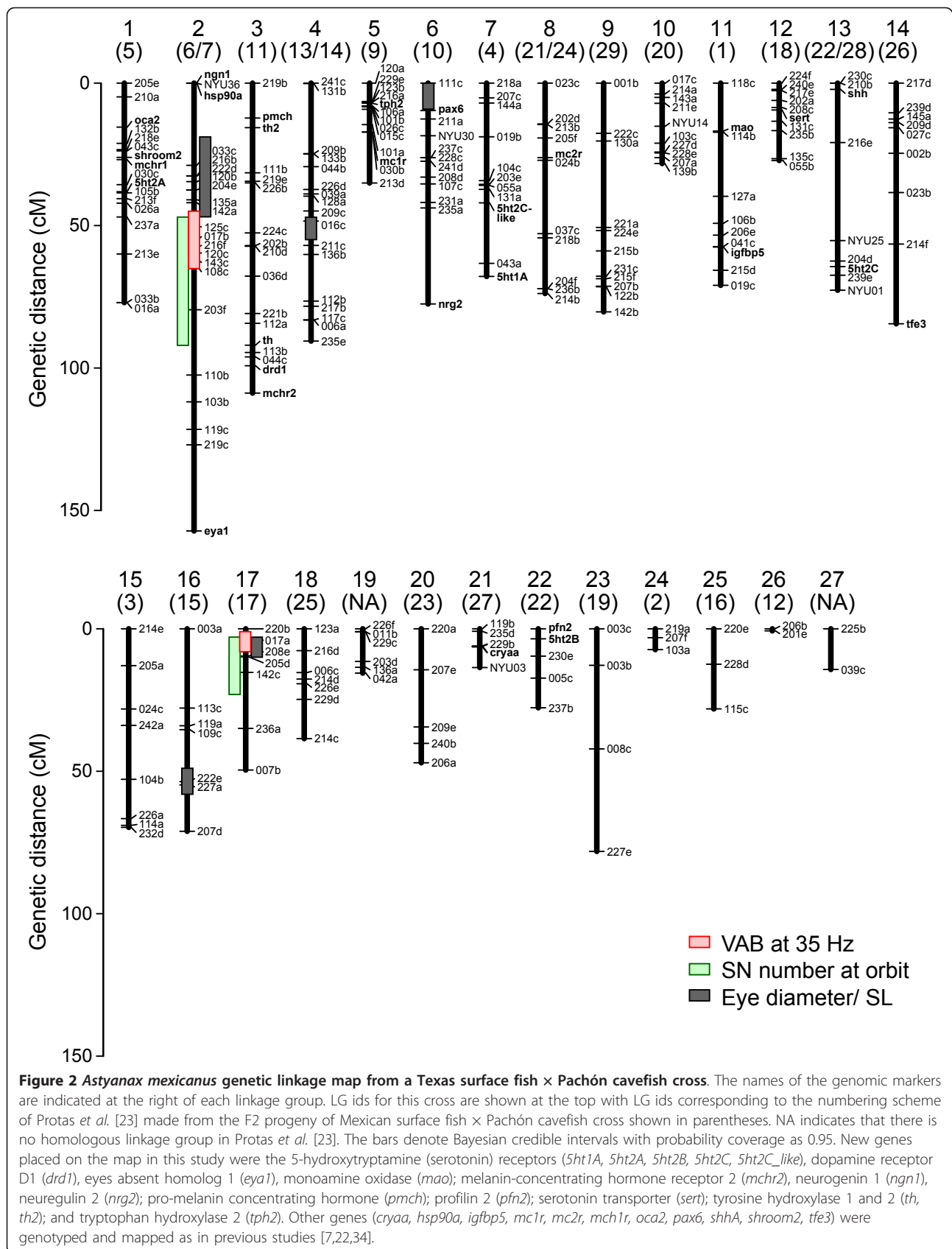


Figure 1 Genetic analysis of VAB, SN and eye regression. (A-E) Histograms showing (A) VAB level (square-rooted number of approaches, or NOA), (B) SO-3 SN number, (C) EO SN number, (D) SO-3 SN diameter, and (E) eye diameter in surface fish, cavefish and their F₁ progeny (upper frames), and the F₂ and F₃ generations (lower frames). The F₁ and F₂ phenotypes are intermediate between surface fish and cavefish, and the sum of F₂ and F₃ phenotypes covered most of the range of phenotypes for each trait between surface fish and cavefish, although the distributions of SO-3 and EO SN numbers remain somewhat restricted towards the surface fish phenotype. (F-G) Regression analysis showing the relationships between VAB and (F) EO SN number, (G) SO-3 SN number, (H) SO-3 SN diameter, and (I) eye diameter/SL. (J) The relationship of SN number at EO and eye diameter/SL. EO SN number and SO-3 SN diameter were both positively correlated with VAB level, which was negatively correlated with eye size. EO SN number was also negatively correlated with eye size. Linear regression lines are shown in red. (K-N) Bright field images (upper) and DASPEI-stained neuromasts (lower) compared among (K) surface fish, (L-M) two examples of F₃ hybrids, and (N) cavefish. Scale bar in (N) is equal to 1.0 mm. In K-N, circles outlined by white dashed lines indicate the edges of the eye, red dashed lines indicate the lines of suborbital canal neuromasts in the head lateral line, the areas enclosed by the blue dotted lines indicate the approximate outline of the SO-3 region, and the areas shown by the yellow dotted lines and indicated by yellow arrows show the EO regions.



QTL for albinism at the *oca2* gene locus on LG1 [23] (Table 1, Additional file 1F, G) and for eye size on LG 2 [33]. We conclude that we can safely drop relatedness for the remaining traits and, therefore, show the results for multiple QTL mapping using the combined F₂ and F₃ datasets.

Two QTL for cavefish VAB at 35 Hz but not other frequencies

We initially surveyed QTL for VAB at different vibration stimuli. As reported previously, cavefish show the strongest VAB at 35 Hz and intermediate-levels at 10 and 50 Hz; additionally, some surface fish show an intermediate-level of VAB at a broad range between 5 and 35 Hz [27,40]. By performing an abbreviated QTL scan using the single-QTL model, we detected two significant QTL for VAB, but only with the 35 Hz stimulus (Figure 3A). This indicates that cavefish VAB at 35 Hz has a genetic basis. The same VAB QTL were revealed using *stepwiseqtl* mapping below.

Two QTL clusters control VAB, EO SN number and eye size

By performing *stepwiseqtl*, we detected nine QTL: two each for VAB and EO SN number on LG 2 and 17, and five for eye size on LGs 2, 4, 6, 16, and 17 (Figure 3, Table 1). The QTL for VAB and EO SN number were relatively consistent across all types of analyses, allowing for some variation since single-QTL models are not designed to detect QTL for complex traits. The eye size QTL on LG 2 and 17 were also consistent among analyses, but the eye QTL on LG 4, 6 and 16 were not evident in the single-QTL scans (Additional file 1B, left column). Although this result may be expected since eye size is genetically complex in *Astyanax*

[33], these three QTL will need to be confirmed in future analyses. We did not detect significant epistasis among any of these QTL (Figure 3, Table 1). For each phenotype, the sum of detected QTL accounted for 19.8%, 18.5% and 40.1% of the total phenotypic variance in VAB, EO SN number and eye size, respectively (Table 1). Although the QTL for these three traits were found on five different linkage groups distributed throughout the *Astyanax* genome, the Bayesian credible intervals for six VAB, EO SN and eye size QTL formed congruent or overlapping clusters on LGs 2 and 17 (1 cM overlap at the 47 cM position in LG 2, and 5 cM overlap at the 3 to 8 cM position of LG 17; Figures 2 and 3B, C). Particularly noteworthy, the credible intervals for the two most significant eye size QTL overlap with the two QTL for VAB and EO SN number (Figure 3B, C). The observed number of QTL clusters for these three traits is significantly higher than expected by under a Poisson distribution ($X^2 = 98.2$, $df = 3$, $P = 3.8 \times 10^{-21}$) [47]. Since alleles located within short genomic regions are generally inherited together as a unit, these QTL clusters support the physical correlations we found for VAB, EO SN number and eye size (Figure 1F, I, J).

Further examination of these overlapping QTL supports the hypothesis that VAB is enhanced by expanding the number of SN within the EO at the cost of eyes. We found that the cavefish alleles at each QTL shift the VAB, SN and eye size phenotypes in the direction expected given the distribution of these phenotypes between the surface fish and cavefish P₀; when VAB level was high there were more SN and smaller eyes than when VAB level was low or absent (Table 1; see insets of Figure 3B, C; and Additional file 3). None of the 28 candidate genes were associated with any of the

Table 1 A summary of the location and effect size of significant QTLs for six traits

Trait	N	Linkage Group	Position	LOD	PVE	Effect size and direction
VAB	227				Total: 19.79	√NOA (0 to 7.68)
		2	51.0	3.85	6.52	+1.11
		17	4.0	5.69	9.81	+1.22
EO SN number	253				Total: 18.54	SN number (0 to 10)
		2	75.0	5.74	8.98	+2.02
		17	8.0	3.84	5.89	+1.51
Eye diameter/SL	350				Total: 40.13	Eye-size/SL (0.0558 to 0.1382)
		2	28.9	10.22	8.62	-0.0128
		4	48.4	4.93	4.01	+0.0068
		6	4.0	5.44	4.44	-0.0065
		16	54.0	7.83	6.50	-0.0078
Albinism	254					Albino (0) - Pigmented (1)
		1	16.0	55.91	63.71	-0.86

N is the number of F₂ and F₃ individuals used, LOD is the log of odds ratio, and PVE is the percentage of phenotypic variance explained. The summed PVE of all QTL are shown at the top row of each trait (at Total). Effect size and direction (positive and negative) of QTL refers to the magnitude of shift between homozygotes of surface fish alleles and cavefish alleles. The numbers in parentheses indicate the ranges of phenotypes. Three QTL for eye diameter/SL at LG 4, 6 and 16 require further analyses to be confirmed (see Results).

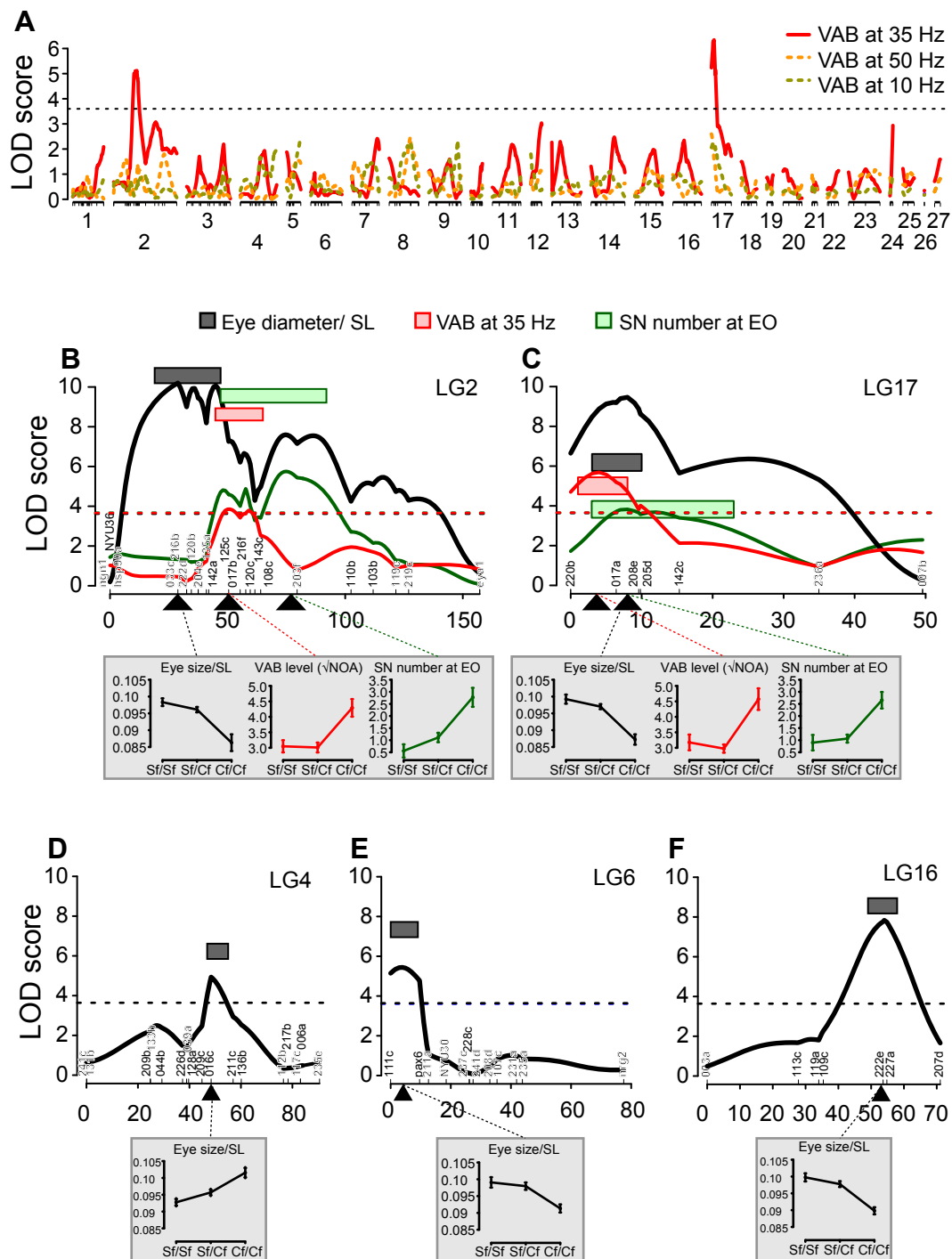


Figure 3 QTL mapping of VAB, SN number and size, and eye size. (A) LOD scores computed with single-QTL model genome-scan are plotted against the distance across each linkage group (LG). Red solid lines indicate LOD scores for VAB-level at 35 Hz vibration stimulus, yellow dotted lines for VAB at 50 Hz stimulus, and lime green dotted lines for VAB at 10 Hz stimulus. Significant VAB QTL were detected at LG2 and 17 only at 35 Hz stimulus. The horizontal line indicates the genome-wide significance thresholds at $P < 0.05$. (B, C) LOD scores computed following multiple QTL mapping. Nine QTL were found across five different LG (see also Table 1). Six overlapping Bayesian credible intervals of QTL for VAB, EO SN number and eye size were found on LG 2 and 17. The X-axis indicates genetic distance in centimorgans (cM), and colored bars denote Bayesian credible intervals with probability coverage as 0.95 for each significant QTL. Insets with gray background show effect plots of phenotypic values against each genotype (mean \pm s.e.m.) at the peak locus denoted by the black triangle. *Sf/Sf*, surface fish homozygote, *Sf/Cf*, heterozygote, and *Cf/Cf*, cavefish homozygote. Horizontal dotted lines are genome-wide significant thresholds ($P < 0.05$) calculated from the single-QTL model (see Methods).

9 QTL. As reported previously [7,33], the *shhA* locus was not located in or near any of the eye size QTL (see at LG13 of Figure 2). In addition, *alphaA crsytallin* (*cryaa*) and *shroom2*, which were located within eye QTL in a previous study [3], did not map to an eye size QTL in the present analysis. The significant clustering of VAB, EO SN and eye size QTL on LG 2 and 17 supports the conclusion that the genetic factors responsible for VAB and EO SN enhancement are also responsible for eye regression, either as a result of genetic hitchhiking or pleiotropy.

The EO SN are major receptors for VAB

The results of the quantitative genetic analyses suggest that VAB and EO SN number are phenotypically and genetically linked to eye size in *Astyanax* cavefish. These results raise the intriguing possibility that VAB is facilitated by an increase in EO SN in cavefish. To test this hypothesis, we compared the level of VAB among cavefish whose area of EO or SO-3 SN were ablated. Following EO SN ablation, cavefish showed a significant decrease in VAB (paired *t*-test: $t_9 = 3.66$; $P = 0.005$; Figure 4A, D; ablated areas in the EO region are shown in Figure 4B; EO SN numbers before ablation are shown in Figure 4C). In contrast, cavefish showed only a minor reduction in VAB following ablation of SO-3 SN, which was not significant (paired *t*-test: $t_6 = 0.68$; $P = 0.524$; Figure 4D). Although the EO SN ablation included a part of the SO-3 region, as well as some canal neuro-masts (Figure 4B), EO SN were consistently removed, whereas SO-3 ablation removed more SN than the total number of EO SN (number of ablated SN in the EO SN ablation: 38.5 ± 7.8 ; in the SO-3 SN ablation: 98.0 ± 27.1 ; mean \pm s.e.m.; $t_{15} = -2.45$, $P = 0.027$). Thus, even though cavefish have fewer EO SN than SO-3 SN, these ablation experiments provide strong evidence that SN in the EO area are the main sensory receptors responsible for VAB.

shh-mediated eye degeneration is insufficient to facilitate VAB and EO SN

Although the genes that increase VAB and EO SN may drive eye regression through genetic hitchhiking or pleiotropy (see also Figure 1I, J), it is still possible that reduced eye size alone may increase VAB. To test this alternative possibility, we further compared the level of VAB among surface fish with experimentally regressed eyes following *shhA* overexpression [26]. In addition to eye size, expanded *shh* expression is also known to increase jaw width and taste bud number in cavefish [11], suggesting that this pathway could potentially alter SN number or VAB. Following *shhA* mRNA overexpression, eye diameter varied considerably among surface fish (horizontal axis on Figure 5A-D), but was not associated with a

significant increase in VAB ($r = -0.12$, $P = 0.53$), EO SN ($r = 0.00$, $P = 1.00$), or SO-3 SN ($r = 0.20$, $P = 0.29$) (Figure 5B-D). These results suggest that *shh*-induced eye regression is insufficient to increase EO SN and VAB and that the molecular pathway decreasing eye size concomitantly with VAB and EO SN enhancement is parallel to the SHH pathway. We conclude that the same or closely linked genetic factors responsible for the enhancement of EO SN and VAB are also responsible for the reduction in eye size (Figure 6).

Discussion

We have shown that eye regression in *Astyanax* cavefish is phenotypically and genetically correlated with the evolution of VAB, an adaptive trait controlling feeding efficiency [27], as well as the enhancement of its sensory receptors, SN specifically localized within the EO. Genetic mapping studies revealed clusters of congruent or overlapping QTL on LG 2 and 17 that control eye size, VAB and the number of EO SN. In addition, we have also demonstrated a significant role of the EO SN in VAB, and that the open space created by *shh*-induced eye degeneration is insufficient to promote VAB or SN enhancement. This experimental result further highlights the importance of the genetic linkage between eye loss and the VAB sensory system. Our results support the hypothesis that selection for an adaptive behavior and its underlying sensory receptors are enhanced in cavefish at the expense of eyes. To our knowledge, this is the first study to report phenotypic and genetic relationships between a regressive phenotype, an adaptive behavior and the sensory system responsible for this behavior.

We have discovered a significant genetic correlation between VAB and EO SN number but not between VAB and SO-3 SN number and size. This result was surprising in light of our previous studies, which found that removal of SO-3 SN reduced (but did not eliminate) VAB [27]. A possible explanation for this discrepancy is that the physical SN ablation method used in our previous study did not discriminate effectively between EO SN and SO-3 SN, which are present in adjacent regions in the cavefish cranium, or that the actual contribution of SO-3 SN to VAB is minor compared to that of EO SN. Our current ablation study supports either explanation by showing that EO SN are the major VAB receptors, whereas SO-3 SN, despite their larger number, have only a minor role in VAB (Figures 1 and 4). Although our EO SN ablation experiment also ablated some SO-3 SN and canal neuro-masts, we conclude that the latter receptors play a minor role in VAB for two reasons. First, in the SO-3 SN ablation experiment, more SN were ablated than EO SN. Yet, despite the loss of more SN in SO-3, the level of VAB was not attenuated significantly (Figure 4). In contrast, deleting a much smaller population of EO SN resulted in a

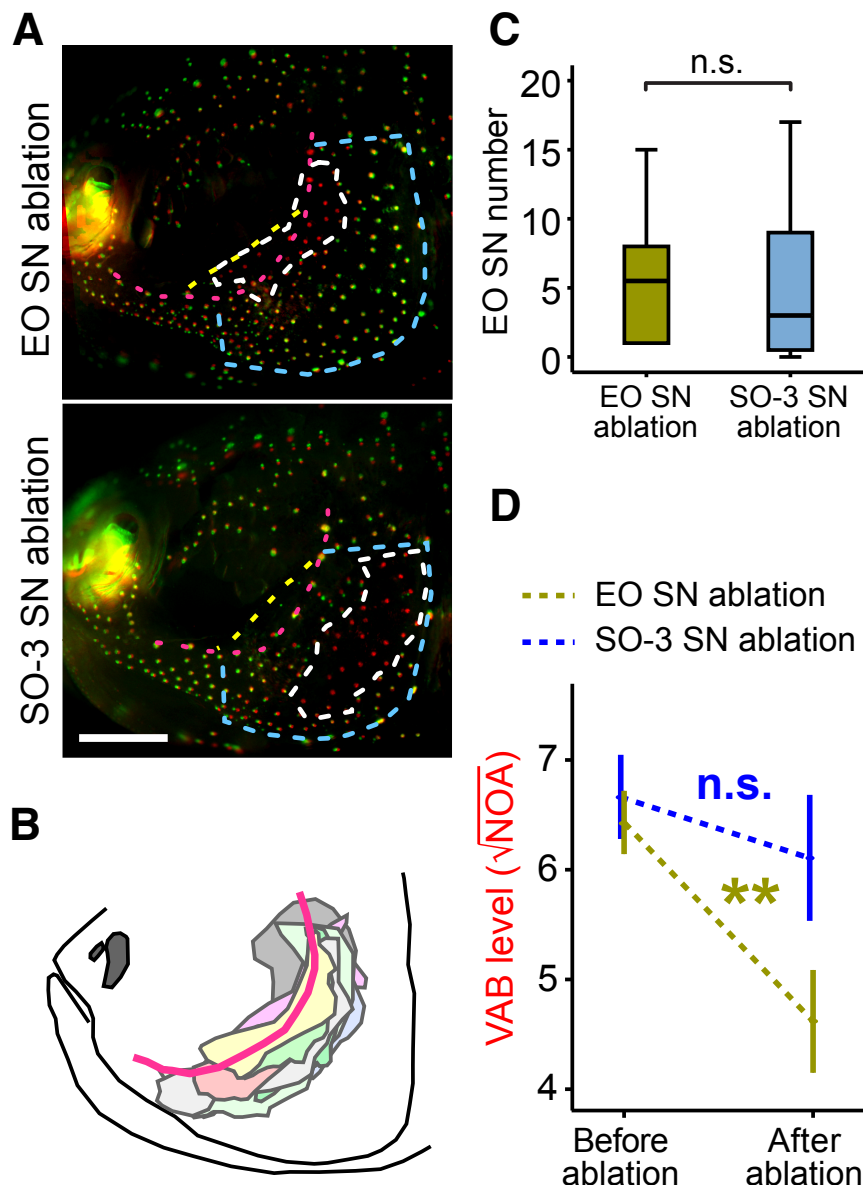


Figure 4 Effects of bilateral SN ablation on VAB in cavefish. (A) Comparison of DASPEI-stained EO SN and SO-3 SN in the ablated areas. The SN present before but absent after ablation within the two ablated regions (outlined by dashed white lines) are pseudo-colored in red. The red dashes indicate the line of suborbital canal neuromasts in the head lateral line and the areas enclosed by the blue dashed lines indicate the SO-3 region; the areas between the suborbital canal lateral line (red dashes) and dashed yellow lines represent the region containing EO SN. Scale bar in (lower panel of A) is 1.0 mm. (B) Schematic drawing of the ablated areas of 10 cavefish in the EO SN ablation experiment. Each experiment was color-coded. The snout is shown at the left. The ablated area included both the EO region and a part of the SO-3 region. The suborbital canal lateral line is indicated with red line. (C) The EO SN number of cavefish prior to ablation of EO or SO-3 SN. There was no difference in EO SN number between these two groups ($Z = -0.54$, $P = 0.614$; $n = 10$ for EO SN ablation; $n = 7$ for SO-3 SN ablation). (D) VAB in cavefish before SN ablation and four to six days after SN ablation. Values are means \pm s.e.m. **: $P < 0.01$. n.s.: not significant. Number of cavefish used were: $n = 10$ for EO, $n = 7$ for SO-3. Rod vibration at 35 Hz was used to measure VAB.

dramatic and statistically significant reduction in VAB (Figure 4). Second, in several former studies, the involvement of canal neuromasts in VAB was excluded through three observations: (1) selective SN ablation was enough to decrease VAB even while maintaining canal neuromasts [27], (2) cavefish VAB was tuned to the frequency at the

peak sensitivity of SN but not of canal neuromasts [27], and (3) the selective interference with canal neuromasts failed to attenuate the response [37]. So what makes EO SN necessary for VAB? It is possible that there are structural or neural circuitry differences between the two populations of EO and SO-3 SN that may account for our

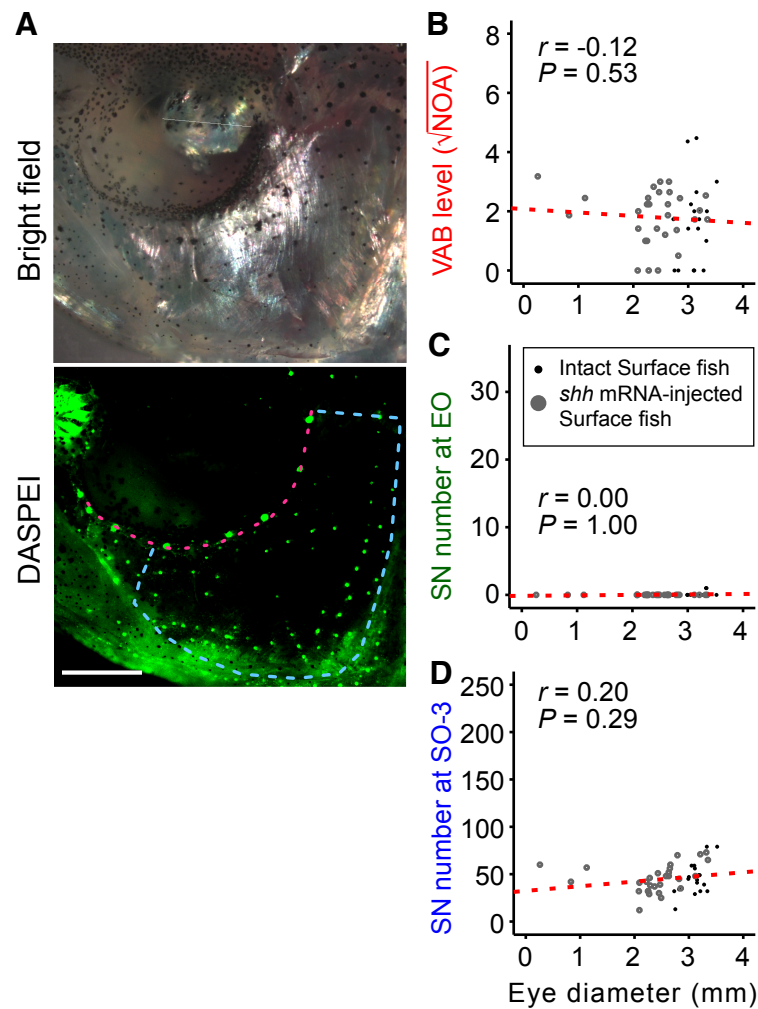
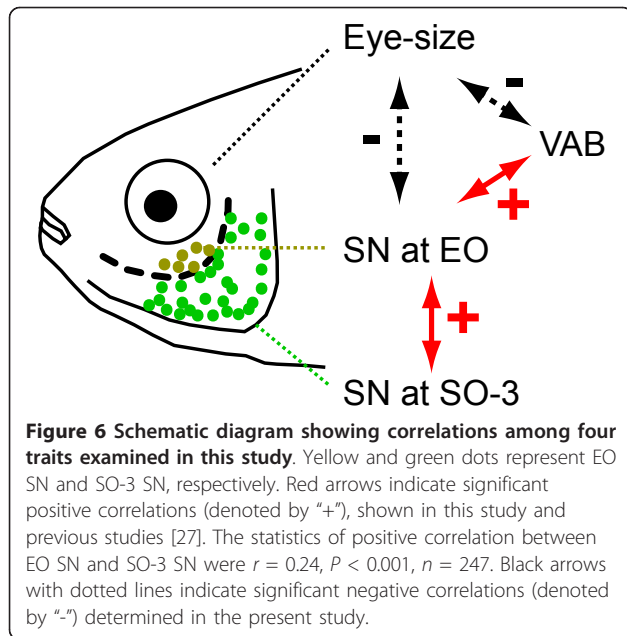


Figure 5 Effects of *shh* induced eye degeneration on VAB and SN number. **(A)** Bright field image (upper) and DASPEI-stained neuromasts (lower) in two-year-old adults that developed from *shhA*-mRNA injected surface fish embryos. The red dashes indicate the line of suborbital canal neuromasts in the head lateral line and the areas enclosed by the blue dashed lines indicate the SO-3 region. Scale bar in (lower panel of A) is 1.0 mm. **(B-D)** Regression analysis showing the relationship between eye diameter and **(B)** VAB level, **(C)** EO SN number and **(D)** SO-3 SN number in *shhA*-mRNA injected surface fish (gray dots) compared to uninjected surface fish (black dots). Linear regression line is shown in red. Eye degeneration did not result in the appearance of SN in the EO or increase VAB level in *shh*-overexpressed surface fish.

results, or that the EO SN are better positioned above the eye socket to detect fluctuations in water due to the bulging shape of the adipose tissue plug that fills the eye orbits of cavefish [5] or bulging eye balls of F_2 and F_3 hybrids [48]. However, since the level of VAB did not drop to zero in our EO SN ablation, it seems likely that other SN contribute to VAB as well, possibly including SN at SO-3 and on the dorsal trunk [27].

Our present investigation has also clarified the difference between the strong type of VAB observed in cavefish (10+ approaches towards a vibrating object) and the weaker form previously detected in a small proportion of surface fish raised in the laboratory (> 4 approaches) [27,40]. Cavefish VAB peaks at 35 Hz, whereas surface fish VAB shows a continuous low activity from 5 to 35

Hz [27,40]. In this study, VAB showed two genetic components detectable at 35 Hz, but none at 10 or 50 Hz, suggesting that the weak form of surface fish VAB appears without a major genomic change and could be accomplished through environmental effects and/or developmental plasticity. Considering that at least three cavefish populations (Pachón, Los Sabinos and Piedras cavefish) exhibit a strong form of VAB [27,49], VAB may, therefore, represent a broadly distributed evolutionary trait in cavefish. The elaboration of SN at a new site, the EO, could have been a key factor in the evolution of VAB during adaptation to subterranean habitats [10,40]. Determining the mechanisms underlying EO SN development and VAB among independently evolved cave populations [50,51] could open a path to



understanding the origins of neurological and behavioral novelty during evolution.

The major conclusions of this study are that EO SN number is strongly correlated with both VAB and eye size, and that all three traits are controlled by QTL on LGs 2 and 17 with congruent or overlapping Bayesian credible intervals. These results suggest that the gene loci responsible for VAB, EO SN number and eye-size may be subject to possible physical linkage and genetic hitchhiking or may in fact be the same genes with pleiotropic effects. The existence of QTL clusters could facilitate rapid adaptation to environmental changes by concurrently fixing multiple beneficial traits. Previous QTL analyses have also shown tight linkages and overlapping QTL for several other cavefish traits, including eye size, lens size, taste bud number, tooth number, melanophore number and chemical sense ability [7,33]. This observation suggests that adaptation to cave life in *Astyanax* is the result of tradeoffs among many phenotypic traits, possibly through functional shifts within pluripotent neural crest cells which contribute to most of the above traits through developmental processes [52]. However, one must note that widespread clustering of QTL does not necessarily entail a phenotypic tradeoff. In a previous scan of QTL in *Astyanax*, Protas et al. reported the overlap of six QTL for eye size and melanophore number (MelE), yet the phenotypic correlation between these traits is only $r = -0.05$ [7,33].

The present investigation provides a clear example of a tradeoff between constructive traits (VAB and EO SN) and a regressive trait (eye size) in parallel to the SHH-signaling pathway. The short genomic distance between the QTL for eye regression, EO SN and VAB [11] could

be a key factor in promoting the rapid adaptation of *Astyanax* to a novel environment. In other rapidly evolving animals, such as African cichlids and three-spined sticklebacks, QTL clusters have also been shown to control groups of potentially advantageous traits, including sex determination and body color, and body shape and plate number [53,54].

Conclusions

We have discovered a significant genetic correlation among eye size, VAB and EO SN number. Our results, therefore, support the hypothesis that eye loss has evolved in *Astyanax* cavefish as a result of indirect selection against eyes due to a trade-off between two constructive traits, VAB and EO SN enhancement, based either on genetic hitchhiking or pleiotropy. There has been a long-standing debate on the neutrality or benefit of eye regression in cave animals [1,2,4,34,35]. Since cave-adapted arthropods exhibit reduced eyes and elongated sensory antennae [1,2,8], the loss of eyes as a result of selection for increased tactile sensitivity is an attractive general hypothesis for the convergent evolution of eye regression in cave fauna.

Methods

Biological materials and crosses

Astyanax mexicanus surface fish used in this study were laboratory raised descendants of original collections made in Balmorhea Springs State Park, Texas, and cavefish were laboratory raised descendants of original collections from Cueva de El Pachón (Pachón cavefish) in Tamaulipas, Mexico. We generated all hybrid progeny from an original mating between one pair of cavefish and surface fish [11,41,55,56]. One pair of F₁ hybrids from this cross was mated to generate 384 F₂ individuals for phenotypic and genetic analysis, while another pair of F₁ hybrids was crossed to generate a second group of about 200 F₂ progeny. These F₁ hybrids were randomly selected. We genotyped this second set of hybrids at markers 017a, 215d, 145a, 204d and 218e, which are near potential VAB (017a and 215d) and SN (145a, 204d and 218e) loci identified by a preliminary QTL scan using 384 F₂ individuals. To overcome a reduced rate of spawning in this group, we chose three pairs of F₂ progeny that were either homozygous or heterozygous for the cavefish alleles at the marker loci and crossed them to generate 91 F₃ progeny. Although these hybrids exhibited a reduced rate of spawning, there was no noticeable difference in their survivability. Hybrids were fed living *Artemia* larvae and were maintained individually in 500 ml tanks or in groups of approximately 10 in 3 L tanks. We phenotyped each hybrid once for SN number and eye size and two or three times for VAB when they were one to two years old. Because of the limitations of tank size

[57], hybrids of different ages approximate the same standard length (approximately 3 cm) and there is no positive relationship between age and SN number at either SO-3 or the EO (Additional file 4). Additionally, the results of our QTL scans did not differ when including age as a covariate (data not shown). The animal procedures used in this study were approved by the University of Maryland Animal Care and Use Committee and conform to NIH guidelines.

Marker genotyping

We isolated genomic DNA from fin-clips using the DNeasy Blood & Tissue Kit (Qiagen, Valencia, CA, USA) or the quick extraction protocol [58]. We genotyped fish for 226 genome-wide polymorphic microsatellite loci described previously [23] and for polymorphisms within or near 20 candidate genes for SN number and behavioral variation. We successfully genotyped 93,208 (95.6%) of these microsatellite markers among 382 F₂ and 11,375 (95.5%) of 125 selected microsatellite markers among 91 F₃. Candidate gene homologues were identified in the fugu, medaka, stickleback, tetraodon and zebrafish genomes. Degenerate primers were designed to match the most conserved amino acid regions using CODEHOP [59] or SCPrimer [60]. We performed degenerate PCR on genomic DNA extracted from the fin-clips of P₀ surface fish and Pachón cavefish using Takara LA Taq DNA polymerase (Clontech, Mountain View, CA, USA) and the following touch-down program: 1 cycle at 94°C for 90 sec; 3 cycles each at 94°C for 20 sec, 63°C for 20 sec and 68°C for 2.5 minutes; 3 cycles each at 94°C for 20 sec, 61°C for 20 sec and 68°C for 2.5 minutes; 3 cycles each at 94°C for 20 sec, 59°C for 20 sec and 68°C for 2.5 minutes; 30 cycles at 94°C for 20 sec, 57°C for 20 sec and 68°C for 2.5 minutes; and finally 1 cycle at 72°C for 4 minutes, followed by a 4°C incubation. PCR fragments were characterized by either direct sequencing with the same degenerate primer used for PCR or by conventional sequencing after sub-cloning into the pCRII plasmid using the TOPO TA Cloning Kit (Invitrogen, Grand Island, NY, USA). The homology of each candidate gene fragment was confirmed by blastn. After sequencing each candidate gene region in surface fish and Pachón cavefish, the sequences were extended with primers designed from known sequences using the GenomeWalker™ Universal Kit (Clontech), and aligned using either Vector NTI (version 7, InforMax, Bethesda, MD, USA) or Sequencher™ (version 5, Gene Codes Corp., Ann Arbor, MI, USA) software to identify microsatellite and single nucleotide polymorphisms (SNPs). Microsatellite polymorphisms were genotyped as described by Protas *et al.* [23] after designing primers in Primer3Plus [61]. SNPs were genotyped by either Taqman® (Roche Applied Science, Indianapolis, IN, USA) or HybProbe (Roche

Applied Science) technology. Primers and fluorescent probes were designed using Primer Express (version 3.0, Applied Biosystems, Carlsbad, CA, USA) or LightCycler® Probe Design Software 2.0 (Roche Applied Science), respectively. The primer and probe sequences for these candidate genes are provided in Additional file 5.

Vibration attraction behavior

We assayed VAB as described previously [27,49]. Briefly, four or five days before the beginning of an assay, individuals were acclimated in a cylindrical assay chamber (Pyrex 325 ml glass dish, 10 cm diameter × 5 cm high, Corning, Corning, NY, USA) filled with conditioned water (pH 6.8; conductivity approximately 600 µS). During the assays, vibration stimuli were created using a 7.5 mm-diameter glass rod vibrating at 35 Hz using a Leader LG1301 function generator (Leader Instruments Corp., Cypress, CA, USA) with an audio speaker (Pro Speakers, Apple, Cupertino, CA, USA). The number of approaches (NOA) to the vibrating rod was video recorded during a three-minute period under infrared illumination (880 nm wave length, BL41192-880 black light, Advanced Illumination, Rochester, VT, USA), and counted using ImageJ 1.42q software (NIH, Bethesda, MD, USA).

Eye measurements

Eye size was determined from photographs of each fish by digitally measuring the diameter of each eyeball along its rostral-caudal axis using ImageJ. We standardized these measurements by dividing them by each fish's standard length (SL), the length of the body from the tip of the snout to the base of the caudal fin.

Neuromast vital staining

Neuromasts were vital stained as described previously [27,49]. Briefly, fish were immersed in 25 µg/ml 2-(4-(dimethylamino)styryl)-N-ethylpyridinium iodide (DASPEI; Invitrogen, Eugene, OR, USA) [62] dissolved in conditioned water for one hour, followed by immersion in ice-cold 66.7 µg/ml Ethyl 3-aminobenzoate methane-sulfonate salt (MS222, Sigma) in conditioned water. The specimens were viewed under a fluorescence microscope (Axioskop 2 equipped with 2.5× Plan-Neofluar lens with a numerical aperture of 0.075 and a FITC filter set; Zeiss, Göttingen, Germany); we then photographed the fish with a Zeiss Axiocam CCD camera. Neuromasts were quantified on images of DASPEI-stained fish using ImageJ software. SN were counted both in the epidermis over the cranial third suborbital (SO-3) bone [41] and within the orbit epidermis dorsal to the line of the suborbital canal neuromasts (indicated by red dashed line in Figure 1L-N). To determine SN size, the long diameter of the 10 largest SN in the same area was measured and averaged.

Linkage and QTL mapping

Following marker genotyping, we used MapManager QTXb20 [63] software to construct an initial linkage map of the SNP and microsatellite markers using 384 F₂ fish with complete genotype data and the Kosambi map function. We then used the program R/qtl [45] to identify statistically unlikely events, such as double crossovers in adjacent intervals or single crossovers in a small interval under maximum likelihood estimation [64], to refine marker order and to estimate inter-marker distances.

We performed QTL mapping using two strategies: (1) multiple interval mapping via the function *stepwiseqtl* in R/qtl [45]; and (2) single-QTL model mapping accounting for relatedness in the program QTLRel [44]. All logarithms of the odds (LOD) significant thresholds were determined following 2,000 permutation tests after single-QTL model mapping with *scanone* implemented in R/qtl or *scanOne* in QTLRel. The 95% Bayesian credible intervals for QTL positions, which are analogous to 95% confidence intervals, were obtained using R/qtl. For multiple QTL mapping, we first calculated genotype probabilities for any missing genotype using the *calc.genoprob* function before performing the forward/backward model selection function implemented in *stepwiseqtl*. Following model selection, we chose the model with the maximum penalized LOD score generated from 1,200 permutation tests [65]. For QTLRel mapping, we first generated pedigree charts for the F₂ and F₃ hybrid families and then calculated condensed identity coefficients and estimated variance components with the *cic* function. We used these variance components when scanning the genome for QTL using the *scanOne* function (see Additional file 2). The genome-wide significant thresholds ($P < 0.05$) for this latter analysis were calculated from 2,000 permutation tests.

SN microablation

SN were ablated by a modification of our previous method [27]. Prior to ablation, we measured VAB and counted neuromasts stained with DASPEI. Only cavefish showing a high VAB level (more than 16 NOA) were selected for SN ablation. SN were ablated by applying Vetbond non-toxic tissue adhesive (3M, St. Paul, MN, USA) either to the EO or the SO-3 region using a micro nylon loop, a traditional embryological tool [58]. After application of tissue adhesive to one side, cavefish were exposed to air for 10 seconds, and tissue adhesive was then applied to the same area on the opposite side, followed by a second cycle of air-drying. The treated fish were placed in a 10 cm-diameter cylindrical chamber containing conditioned water at room temperature. Within a day of active swimming the tissue adhesive usually peeled off the body, resulting in a void in the underlying field of SN. After four to six days of acclimation/recovery, SN ablated fish were subjected to

the VAB assay followed immediately by staining for one hour with 25 µg/ml DASPEI.

shh overexpression

Overexpression was carried out by injecting zebrafish *shhA* mRNA (20 to 80 pg) into two to four cell stage embryos as described previously [26]. Capped *shhA* mRNA was synthesized from the pSP64T plasmid using the mMESSAGE mMACHINE[®] SP6 Kit (Life Technologies, Grand Island, NY, USA).

Statistics

Correlation studies were conducted using IBM SPSS 20.0.0 software (IBM, Somers, NY, USA). Castle-Wright estimates were performed according to Lynch and Walsh [66]. Significance of QTL clustering was performed using a goodness-of-fit [47]. We divided the 1,500 cM *Astyanax* genome into 50 bins of 30 cM each and counted the number of bins with 0, 1, 2 and 3 QTL. We then compared this observed distribution to that expected from a Poisson distribution where the average number of QTL expected per bin is 0.18 (9 QTL divided by 50 bins of 30 cM each).

Additional material

Additional file 1: LOD scores from single-QTL mapping analyses with or without accounting for relatedness among the F₂ and F₃.

(A-F) LOD scores computed with classic single-QTL interval mapping using the F₂ dataset (blue lines), F₃ dataset (green lines), or F₂ + F₃ combined dataset (red lines) in R/qtl (left column) and QTLRel (right column). In QTLRel, condensed identity coefficients were calculated to adjust background variation according to kinship among the F₂ and F₃ generations. This analyses found (A) two QTL by the classic scan with the F₂ and the F₃ dataset (left column), or one QTL (right column) for VAB, (B) five QTL with the F₂ and the F₃ dataset (left at LG 2, 9, 17 and 23), or three QTL (right at LG2 and 17) for eye-size, (C) one QTL for EO SN number in both, no significant QTL for either (D) SO-3 SN number or (E) SO-3 SN diameter, and (F) one QTL for albinism in the both methods. (G) The LOD score from multiple QTL mapping of albinism also identified a single QTL at the *oca2* locus, as described previously [23]. The horizontal lines indicate genome-wide significance of $P < 0.05$ based on 2,000 permutation tests.

Additional file 2: Variance Components calculated in QTLRel

software. The phenotypes of VAB, Eye size, EO SN number and albinism exhibited small variance components for both the additive and the dominance genetic matrixes, whereas SO-3 SN number and SO-3 SN diameter exhibited large variance components at the dominance genetic matrix. AA: additive genetic matrix; DD: dominance genetic matrix; and EE: the residual matrix.

Additional file 3: Scatterplots of phenotypic values against each genotype at the two cluster loci.

Scatterplots of phenotypic values of VAB (top row), eye size/SL (middle row) and EO SN number (bottom row) were shown at the marker position of 17b (left column, VAB and EO SN number), 222d (left column, eye size), and 17a (right column, all three traits) at linkage group 2 and 17. Blue dots and bars: F₂ generation, Green dots and bars: F₃ generation. Bars indicate mean ± s.e.m. Sf/Sf, surface fish homozygote; Sf/Cf, heterozygote; and Cf/Cf, cavefish homozygote. The cavefish alleles at each QTL cluster shift the distributions of VAB, SN and eye size phenotypes in the direction toward higher VAB level, more EO SN and smaller eyes.

Additional file 4: Phenotypic distributions between approximately one- and two-year-old fish used in current study. The boxplot of phenotypic distributions were compared between approximately one- and two-year-old F₂ fish. The increased VAB levels in two-year-old fish (top) was not associated with the increases of EO (middle; no significant difference: n.s.; The Mann-Whitney non-parametric test was applied since phenotypic values were not normally distributed), or SO-3 SN number (bottom; significantly decreased in two-year-old fish). N were indicated in the boxes.

Additional file 5: Candidate gene primer and probe sets used in this study. Primers for the microsatellite markers were designed to amplify 150 to 350 base-pair genomic fragments containing length polymorphisms between surface fish and cavefish. Primers and fluorescent probes for Taqman and HybProbe genotyping methods were designed to detect single nucleotide polymorphisms between these two morphs.

Abbreviations

DASPEI: 2-(4-(dimethylamino)styryl)-N-ethylpyridinium iodide; EO: eye orbit; LG: linkage groups; LOD: logarithms of the odds; MelE: melanophore number above the eye; NOA: number of approaches; QTL: quantitative trait locus; s.e.m.: standard error of the mean; *shh*: sonic hedgehog; SL: standard length of fish; SN: superficial neuromast; SNPs: single nucleotide polymorphisms; SO-3: suborbital bone 3; VAB: vibration attraction behavior.

Authors' contributions

MY and WRJ conceived the project and designed the experiments. MY performed behavioral assays, vital dye labeling (Dil), morphometrics, cloning, most of the genotyping, QTL mapping, SN ablation studies, and a part of the *shh*-injection experiments and analyses, and generated the figures. YY performed some of the *shh*-injection experiments. KEO participated in the QTL mapping analyses. MY wrote the manuscript with significant contributions from KEO and WRJ. All authors read and approved the final manuscript.

Competing interests

The authors declare that they have no competing interests.

Acknowledgements

We thank Z Sanford, R Fernandez, J Giarrusso, D Norman, S Ahmed, S Siddiqui, L Younger and J Park for fish maintenance; R Fernandez, D Norman, S Ahmed and J Park for genotyping and phenotyping; K Broman for helpful comments on QTL mapping; and A Parkhurst for technical assistance. A Japan Society for the Promotion of Science Postdoctoral Fellowship to MY and NSF (IBN-05384) and NIH (R01-EY014619) grants to WRJ supported this research.

Author details

¹Department of Biology, University of Maryland, College Park, MD 20742, USA. ²Department of Cell and Developmental Biology, University College London, Gower Street, London WC1E 6BT, UK.

Received: 3 October 2012 Accepted: 27 December 2012

Published: 27 December 2012

References

1. Culver DC: *Cave Life, Evolution and Ecology* Cambridge: Harvard University Press; 1982, 189.
2. Culver DC, Pipan T: *The Biology of Caves and other Subterranean Habitats* Oxford: Oxford University Press; 2009, 254.
3. Protas M, Jeffery WR: **Evolution and development in cave animals: from fish to crustaceans.** *Wiley Interdiscip Rev Dev Biol* 2012, **1**:823-845.
4. Darwin C: *On the Origin of Species Based on Natural Selection, or the Preservation of Favoured Races in the Struggle for Life.* 6 edition. London: John Murray; 1859, 480.
5. Wilkens H: **Evolution and genetics of epigeal and cave *Astyanax-fasciatus* (Characidae, Pisces) - support for the neutral mutation theory.** *Evol Biol* 1988, **23**:271-367.
6. Culver DC, Wilkens H: **Critical review of the relevant theories of the evolution of subterranean animals.** In *Ecosystems of the World. Volume 30.* Edited by: Wilkens H, Culver DC, Humphreys WF. Amsterdam: Elsevier; 2000:381-398.
7. Protas M, Conrad M, Gross JB, Tabin C, Borowsky R: **Regressive evolution in the Mexican cave tetra, *Astyanax mexicanus*.** *Curr Biol* 2007, **17**:452-454.
8. Jernigan RW, Culver DC, Fong DW: **The dual role of selection and evolutionary history as reflected in genetic correlations.** *Evolution* 1994, **48**:587-596.
9. Schemmel C: **Vergleichende Untersuchungen an den Hautsinnesorganen ober- und unterirdisch lebender *Astyanax*-Formen.** *Z Morph Tiere* 1967, **61**:255-316.
10. Franz-Odenaal TA, Hall BK: **Modularity and sense organs in the blind cavefish, *Astyanax mexicanus*.** *Evol Dev* 2006, **8**:94-100.
11. Yamamoto Y, Byerly MS, Jackman WR, Jeffery WR: **Pleiotropic functions of embryonic sonic hedgehog expression link jaw and taste bud amplification with eye loss during cavefish evolution.** *Dev Biol* 2009, **330**:200-211.
12. Jeffery WR: **Adaptive evolution of eye degeneration in the Mexican blind cavefish.** *J Hered* 2005, **96**:185-196.
13. Mitchell RW, Russell WH, Elliott WR: In *Mexican Eyeless Characin Fishes, Genus *Astyanax*: Environment, Distribution, and Evolution. Volume 89.* Lubbock, Texas, USA: Texas Tech University Press; 1977.
14. Jeffery WR: **Cavefish as a model system in evolutionary developmental biology.** *Dev Biol* 2001, **231**:1-12.
15. Jeffery WR: **Evolution and development in the cavefish *Astyanax*.** *Curr Top Dev Biol* 2009, **86**:191-221.
16. Jeffery WR: **Emerging model systems in evo-devo: cavefish and microevolution of development.** *Evol Dev* 2008, **10**:265-272.
17. Strecker U, Hausdorf B, Wilkens H: **Parallel speciation in *Astyanax* cave fish (Teleostei) in northern Mexico.** *Mol Phylogenet Evol* 2012, **62**:62-70.
18. Ornelas-García CP, Domínguez-Domínguez O, Doadrio I: **Evolutionary history of the fish genus *Astyanax* Baird & Girard (1854) (Actinopterygii, Characidae) in Mesoamerica reveals multiple morphological homoplasies.** *BMC Evol Biol* 2008, **8**:340.
19. Gross JB: **The complex origin of *Astyanax* cavefish.** *BMC Evol Biol* 2012, **12**:105.
20. Bradic M, Beerli P, Garcia-de Leon FJ, Esquivel-Bobadilla S, Borowsky RL: **Gene flow and population structure in the Mexican blind cavefish complex (*Astyanax mexicanus*).** *BMC Evol Biol* 2012, **12**:9.
21. Gross JB, Borowsky R, Tabin CJ: **A novel role for Mc1r in the parallel evolution of depigmentation in independent populations of the cavefish *Astyanax mexicanus*.** *PLoS Genet* 2009, **5**:e1000326.
22. Menuet A, Alunni A, Joly JS, Jeffery WR, Rétaux S: **Expanded expression of sonic hedgehog in *Astyanax* cavefish: multiple consequences on forebrain development and evolution.** *Development* 2007, **134**:845-855.
23. Protas ME, Hersey C, Kochanek D, Zhou Y, Wilkens H, Jeffery WR, Zon LI, Borowsky R, Tabin CJ: **Genetic analysis of cavefish reveals molecular convergence in the evolution of albinism.** *Nat Genet* 2006, **38**:107-111.
24. Varatharasan N, Croll RP, Franz-Odenaal T: **Taste bud development and patterning in sighted and blind morphs of *Astyanax mexicanus*.** *Dev Dyn* 2009, **238**:3056-3064.
25. Yamamoto Y, Jeffery WR: **Central role for the lens in cave fish eye degeneration.** *Science* 2000, **289**:631-633.
26. Yamamoto Y, Stock DW, Jeffery WR: **Hedgehog signalling controls eye degeneration in blind cavefish.** *Nature* 2004, **431**:844-847.
27. Yoshizawa M, Gorički Š, Soares D, Jeffery WR: **Evolution of a behavioral shift mediated by superficial neuromasts helps cavefish find food in darkness.** *Curr Biol* 2010, **20**:1631-1636.
28. Duboué ER, Keene AC, Borowsky RL: **Evolutionary convergence on sleep loss in cavefish populations.** *Curr Biol* 2011, **21**:671-676.
29. Coombs S, Patton P, Windsor S: **Active wall following by Mexican blind cavefish (*Astyanax mexicanus*).** *J Comp Physiol A Neuroethol Sens Neural Behav Physiol* 2010, **196**:853-867.
30. Sharma S, Coombs S, Patton P, De Perera TB: **The function of wall-following behaviors in the Mexican blind cavefish and a sighted relative, the Mexican tetra (*Astyanax*).** *J Comp Physiol A Neuroethol Sens Neural Behav Physiol* 2009, **195**:225-240.
31. Windsor SP, Norris SE, Cameron SM, Mallinson GD, Montgomery JC: **The flow fields involved in hydrodynamic imaging by blind Mexican cave fish (*Astyanax fasciatus*). Part II: gliding parallel to a wall.** *J Exp Biol* 2010, **213**:3832-3842.

32. Elipot Y, Hinaux H, Callebert J, Rétaux S: **Evolutionary shift from fighting to foraging in blind cavefish through changes in the serotonin network.** *Curr Biol* 2012.
33. Protas M, Tabansky I, Conrad M, Gross JB, Vidal O, Tabin CJ, Borowsky R: **Multi-trait evolution in a cave fish, *Astyanax mexicanus*.** *Evol Dev* 2008, **10**:196-209.
34. Porter ML, Crandall KA: **Lost along the way: the significance of evolution in reverse.** *Trends Ecol Evol* 2003, **18**:541-547.
35. Barr TC: **Cave ecology and the evolution of troglobites.** *Evol Biol* 1968, **2**:35-102.
36. Parzefall J: **Field observation in epigeal and cave populations of Mexican characid *Astyanax mexicanus* (Pisces, Characidae).** *Mém Biospéleol* 1983, **10**:171-176.
37. Abdel-Latif H, Hassan ES, von Campenhausen C: **Sensory performance of blind Mexican cave fish after destruction of the canal neuromasts.** *Naturwissenschaften* 1990, **77**:237-239.
38. Hill LG: **Feeding and food habits of the spring cavefish, *Chologaster agassizi*.** *Am Midl Nat* 1969, **82**:110-116.
39. Eigenmann CH: **Cave Vertebrates of America: a Study in Degenerative Evolution** Washington, DC: The Carnegie Institution of Washington Publications no.104; 1909.
40. Yoshizawa M, Jeffery WR: **Evolutionary tuning of an adaptive behavior requires enhancement of the neuromast sensory system.** *Commun Integr Biol* 2011, **4**:89-91.
41. Yamamoto Y, Espinosa L, Stock DW, Jeffery WR: **Development and evolution of craniofacial patterning is mediated by eye-dependent and -independent processes in the cavefish *Astyanax*.** *Evol Dev* 2003, **5**:435-446.
42. Gross JB, Protas M, Conrad M, Scheid PE, Vidal O, Jeffery WR, Borowsky R, Tabin CJ: **Syntenic and candidate gene prediction using an anchored linkage map of *Astyanax mexicanus*.** *Proc Natl Acad Sci USA* 2008, **105**:20106-20111.
43. Kirby RF, Thompson KW, Hubbs C: **Karyotypic similarities between the Mexican and blind tetras.** *Copeia* 1977, **1977**:578-580.
44. Cheng R, Abney M, Palmer AA, Skol AD: **QTLRel: an R Package for genome-wide association studies in which relatedness is a concern.** *BMC Genet* 2011, **12**:66.
45. Broman KW, Wu H, Sen S, Churchill GA: **R/qtl: QTL mapping in experimental crosses.** *Bioinformatics* 2003, **19**:889-890.
46. Manichaikul A, Moon JY, Sen S, Yandell BS, Broman KW: **A model selection approach for the identification of quantitative trait loci in experimental crosses, allowing epistasis.** *Genetics* 2009, **181**:1077-1086.
47. Albertson RC, Strelman JT, Kocher TD: **Directional selection has shaped the oral jaws of Lake Malawi cichlid fishes.** *Proc Natl Acad Sci USA* 2003, **100**:5252-5257.
48. Rapo MA, Jiang HS, Grosenbaugh MA, Coombs S: **Using computational fluid dynamics to calculate the stimulus to the lateral line of a fish in still water.** *J Exp Biol* 2009, **212**:1494-1505.
49. Yoshizawa M, Ashida G, Jeffery WR: **Parental genetic effects in a cavefish adaptive behavior explain disparity between nuclear and mitochondrial DNA.** *Evolution* 2012, **66**:2975-2982.
50. Wilkens H, Strecker U: **Convergent evolution of the cavefish *Astyanax* (Characidae, Teleostei): genetic evidence from reduced eye-size and pigmentation.** *Biol J Linn Soc Lond* 2003, **80**:545-554.
51. Borowsky R: **Restoring sight in blind cavefish.** *Curr Biol* 2008, **18**:R23-R24.
52. Hall BK: *Evolutionary Developmental Biology*. 2 edition. New York: Springer; 1999.
53. Jones FC, Grabherr MG, Chan YF, Russell P, Mauceli E, Johnson J, Swofford R, Pirun M, Zody MC, White S, Birney E, Searle S, Schmutz J, Grimwood J, Dickson MC, Myers RM, Miller CT, Summers BR, Knecht AK, Brady SD, Zhang H, Pollen AA, Howes T, Amemiya C, Baldwin J, Bloom T, Jaffe DB, Nicol R, Wilkinson J, Lander ES, et al: **The genomic basis of adaptive evolution in threespine sticklebacks.** *Nature* 2012, **484**:55-61.
54. Roberts RB, Ser JR, Kocher TD: **Sexual conflict resolved by invasion of a novel sex determiner in Lake Malawi cichlid fishes.** *Science* 2009, **326**:998-1001.
55. Yoshizawa M, Jeffery WR: **Shadow response in the blind cavefish *Astyanax* reveals conservation of a functional pineal eye.** *J Exp Biol* 2008, **211**:292-299.
56. Jeffery WR, Yamamoto Y: **The lens is a regulator of craniofacial development and evolution in the teleost *Astyanax*.** *Dev Biol* 2000, **222**:239.
57. Gallo ND, Jeffery WR: **Evolution of space dependent growth in the teleost *Astyanax mexicanus*.** *PLoS ONE* 2012, **7**:e41443.
58. Nusslein-Volhard C, Dahm R: *Zebrafish: A Practical Approach* New York: Oxford University Press; 2002, 303.
59. Rose TM, Henikoff JG, Henikoff S: **CODEHOP (Consensus-DEgenerate Hybrid Oligonucleotide Primer) PCR primer design.** *Nucleic Acids Res* 2003, **31**:3763-3766.
60. Jabado OJ, Palacios G, Kapoor V, Hui J, Renwick N, Zhai J, Briese T, Lipkin WI: **Greene SCPrimer: a rapid comprehensive tool for designing degenerate primers from multiple sequence alignments.** *Nucleic Acids Res* 2006, **34**:6605-6611.
61. Untergasser A, Nijveen H, Rao X, Bisseling T, Geurts R, Leunissen JAM: **Primer3Plus, an enhanced web interface to Primer3.** *Nucleic Acids Res* 2007, **35**:W71-W74.
62. Jørgensen JM: **Evolution of octavolateralis sensory cells.** In *The Mechanosensory Lateral Line*. Edited by: Coombs S, Görner P, Münz H. New York: Springer-Verlag; 1989:115-145.
63. Manly KF, Cudmore RH, Meer JM: **Map Manager QTX, cross-platform software for genetic mapping.** *Mamm Genome* 2001, **12**:930-932.
64. Lincoln SE, Lander ES: **Systematic detection of errors in genetic linkage data.** *Genomics* 1992, **14**:604-610.
65. Broman KW, Sen S: *A Guide to QTL Mapping with R/qtl*. 1 edition. New York: Springer-Verlag; 2009, 396.
66. Lynch M, Walsh B: *Genetics and Analysis of Quantitative Traits* Sunderland, Massachusetts, USA: Sinauer Associates, Inc.; 1998.

doi:10.1186/1741-7007-10-108

Cite this article as: Yoshizawa et al: Evolution of an adaptive behavior and its sensory receptors promotes eye regression in blind cavefish. *BMC Biology* 2012 **10**:108.

Submit your next manuscript to BioMed Central and take full advantage of:

- Convenient online submission
- Thorough peer review
- No space constraints or color figure charges
- Immediate publication on acceptance
- Inclusion in PubMed, CAS, Scopus and Google Scholar
- Research which is freely available for redistribution

Submit your manuscript at
www.biomedcentral.com/submit

